A Minituarized Elliptical Patch MIMO Antenna with Low Mutual Coupling for S Band Applications

1st Praveen Kumar
Department of Electronics & Communication Engineering
National Institute of Technology
Jamshedpur, India
2018rsec005@nitjsr.ac.in

1st Arvind Choubey
Department of Electronics & Communication Engineering
Indian Institute of Information Technology
Bhagalpur, India
arvindnit@gmail.com

2nd Ajit Kumar Singh
Department of Electronics & Communication Engineering
Indian Institute of Information Technology
Ranchi, India
ajitsingh31393@gmail.com

1st Rashmi Sinha
Department of Electronics & Communication Engineering
National Institute of Technology
Jamshedpur, India
rsinha.ece@nitjsr.ac.in

2nd Santosh Kumar Mahto
Department of Electronics & Communication Engineering
Indian Institute of Information Technology
Ranchi, India
skumar@iiitranchi.ac.in

ABSTRACT

This paper offers a elliptical patch dual element multiple input multiple output (MIMO) antenna with an impedance bandwidth of 3.35 GHz (2.17-5.57 GHz) using a defected ground structure (DGS) is proposed for S and C-band applications. The proposed DGS structure provides -51.15 dB of isolation at 2.62 GHz and a gap of 10 mm between adjacent antenna elements. The write-up contains a thorough discussion on design, simulation, and performance analysis. Envelope correlation coefficient (ECC) was less than 0.002, diversity gain (DG) greater than 9.99 dB, total active reflection coefficient (TARC) less than 0.35, mean effective gain (MEG) less than -3 dB, and channel capacity loss (CCL) less than 0.3 was achieved. The proposed MIMO antenna is favorable for S-band and C-band applications such as Bluetooth, Wi-Fi, WiMAX, 4G and 5G.

Keywords— DGS, ECC, Isolation, Mutual coupling, MIMO.

I. INTRODUCTION

MIMO antenna can provide high data transfer rates over communication channels in recent generations and the future. MIMO antenna is characterized by high channel capacity [1], the robustness of the communication link [2], high data rate [3], and spectral efficiency [4]. It is typically necessary to keep the space between the near by antenna precisely less to attain compact size. Choosing between closely packed antennas and coupling between them is the foremost task in designing a MIMO antenna. Due to the compactness of the terminals, MIMO systems suffer from the high mutual coupling. Coupling between antennas is an unwanted condition that reduces the antenna's capacity, bandwidth, and efficiency, along with its far-field radiation characteristics [5]. It is therefore important to maintain as much isolation as possible between different antenna elements. Radiating elements can be physically separated by a distance greater than $\lambda/2$ to enhance isolation. In practice, this is impractical for achieving compact antennas.

Numerous isolation enhancement methods are existing in literature in order to overcome the above problem, such as metasurface [6, 7], electromagnetic band gap structure [8, 9], decoupling network [10],

substrate integrated waveguide [11, 12], split ring resonator [13], DGS [14, 15], etc. The periodic structure of the EBG structure, however, makes it a more complex design and a larger structure in size. DGS is the simplest and most convenient mutual coupling reduction technique. In this process, different shapes are etched into the ground plane. There have been different types of shapes proposed for deceasing coupling between nearly placed antenna elements in [14,15].

DGS acts like a band blocking filter analogous to resonant LC circuit. This band-blocking filter is used to block surface waves between nearly placed antennas, thereby reducing the mutual coupling of MIMO systems.

In this paper, two-element MIMO antenna with a simple rectangular slot to the ground and two I-shaped patterns are etched on the ground plane. This I-designed pattern behaves like resonant stubs. The rectangular slot and resonant stubs are presented to enhance the enter-element isolation. The space between the two elliptical patches significantly reduces by 10 mm. The proposed MIMO antenna has a miniaturized size 45 × 48 mm^2 , operating frequency ranging from 2.17-5.52 GHz and maximum isolation -51.15 dB at 2.62 GHz is achieved. The designed MIMO antenna is favorable for S-band and C-band applications for example Bluetooth, Wi-Fi, WiMAX, 4G and 5G.

Section II discusses the precise structure of the design antenna. In sections III, the simulated concert of the antenna is reviewed and described. The performance of the antenna's diversity is covered in Section IV. Section V is the article's conclusion.

II. ANTENNA DESIGN

The layout procedure has been introduced in this section of the proposed MIMO antenna, shown in Figure 1. The development of the novel MIMO antenna has done in two sequential stages. Two elliptical motifs are carved on the substrate in the first step, shown in Figure 1(a). As a result, the patch serves as a radiating element. A rectangular slot is etched in the second stage, followed by two I-shaped stubs being printed on the ground plane. In order to reduce mutual copling between neighboring antennas, the I-shaped stub has been proposed after investigating various structures readily available. The concluding MIMO antenna with I-designed stubs is intended on an inexpensive FR-4 lossy substrate with a thickness of 1.6 mm, dielectric constant (ϵr) = 4.3, and loss-tangent (δ) = 0.025. To improve the isolation and the compactness, an I-shaped stub isolator is printed below the substrate. Simulation has been achieved with the use of HFSS 19.0. The optimized layout characteristics for the MIMO antenna and I-shaped stub are SW=48 mm, SL=45 mm, GL=25 mm, T=13.7 mm, R=11.3 mm, Q=2.1 mm, G=24.65 mm, PW=3 mm, PL=31.1 mm, PC=15.25 mm, b=5mm, and a=9 mm. The front and experimental setup of a fabricated MIMO antenna are shown in Figures 2 (a) and (b). A PNA Microwave Vector Network Analyzer N5222A is used to measure the fabricated MIMO antenna. Figure 2

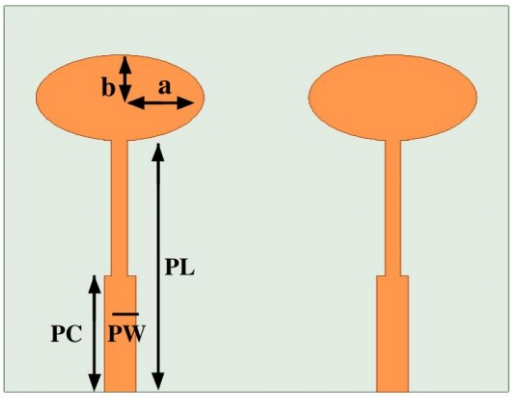

illustrates a typical experimental setup.

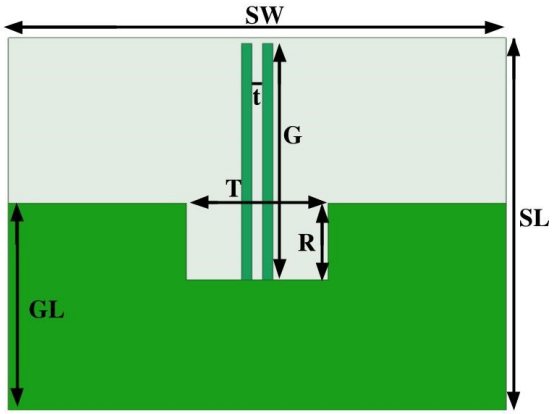

Figure 1. Simulated MIMO antenna (a) front, and (b) back view.

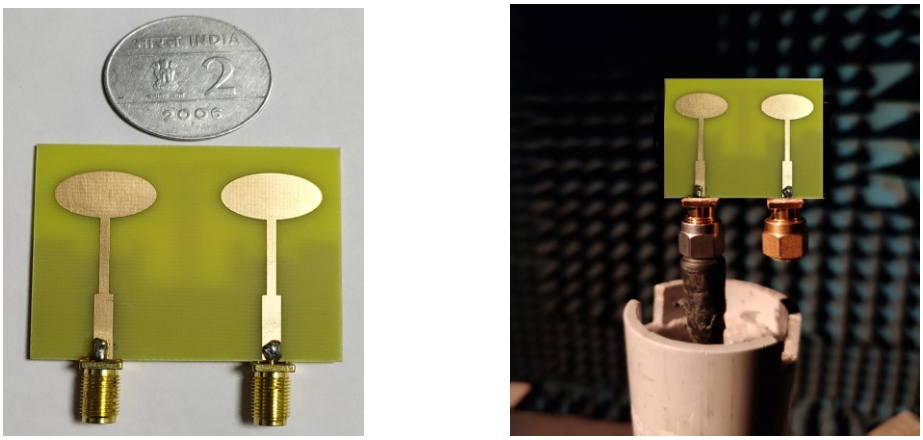

(a) (b)

Figure 2. Fabricated (a) MIMO antenna, and (b) experimental setup.

III. RESULT AND DISCUSSION

In this section, the overall functionality of the designed MIMO antenna is assessed by studying S-parameter, radiation pattern, surface current distribution, and diversity performance consisting of MEG, ECC, DG, TARC, and CCL.

The S_{11} and S_{12} of design MIMO antenna with different development process are depicted in Figure 3. Figure 3(a) & (b) shows the variation of S-parameter characteristics due to rectangular slot in the ground and I-Shaped stubs printed on the ground plane. From Figure 3(a) represents the impedance bandwidth is approximately equivalent in all progress steps. Figure 3(b) shows that if slot is etched to the ground plane, which increases the isolation and further to enhance isolation two I-shaped stubs are included. The designed MIMO antenna with DGS technique is evaluated in three steps partial ground, rectangular slot and stubs.

The MIMO antenna's reflection and transmission coefficient shown in Figure 4. The bandwidth of the proposed MIMO antenna ranging from 2.15 to 5.52 GHz. Throughout the whole bandwidth, mutual coupling less than -20 dB, which shows good isolation between adjacent antenna elements. The peak isolation of the MIMO antenna is -51.15 dB at 2.62 GHz. Analysis of Figure 4 shows that the simulated and experimental results are very close to each other.

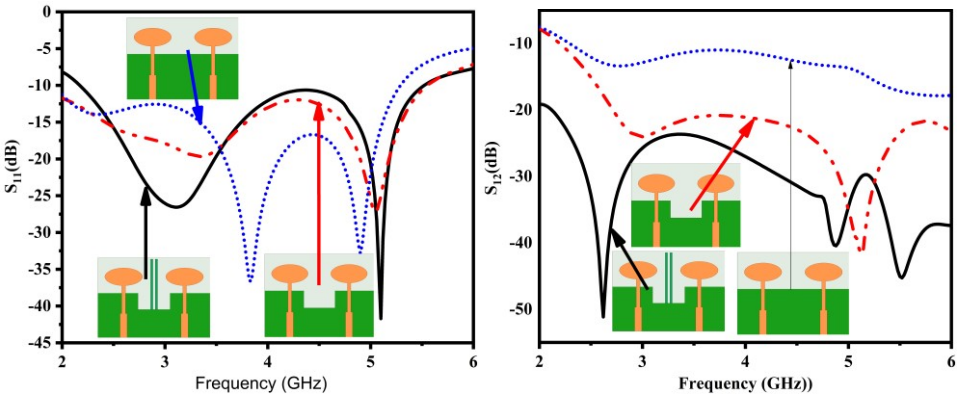

(a) (b)

Figure 3. Evolution steps of (a) Reflection coefficient (S_{11}), (b) Transmission coefficient (S_{12})

.

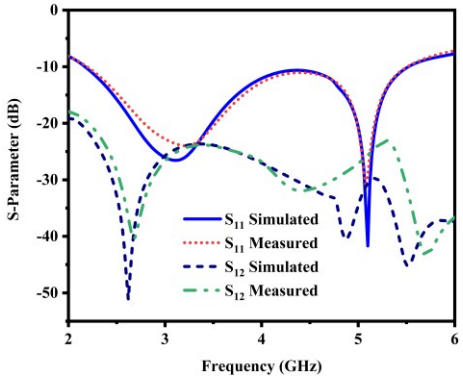

Figure 4. Reflection and transmission coefficient.

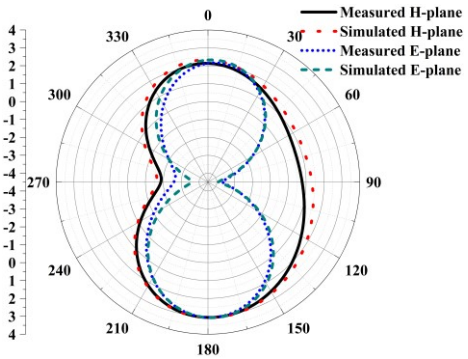

Figure 5. 2-D radiation pattern.

Figure 5 represents the simulated and measured 2D radiation pattern of the proposed two port MIMO antenna at 2.62 GHz and it is noticed that at $\phi = 0°$, pattern is similar to a dipole and omnidirectional at $\phi = 90°$.

The surface current distribution of both antennae with DGS structure is shown in Figure 6. The effect of DGS on surface current can easily be seen by analyzing surface current. When ant-1 is in active mode and ant-2 is equivalent to 50 Ω load, then surface currents flow from port 1 to port 2. As a result, a high surface current is induced on antenna 1, which is captured by the DGS structure. Subsequently, Low mutual coupling between Ant-1 and Ant-2 shows that the designed decoupling technique is good in the desired MIMO antenna applications.

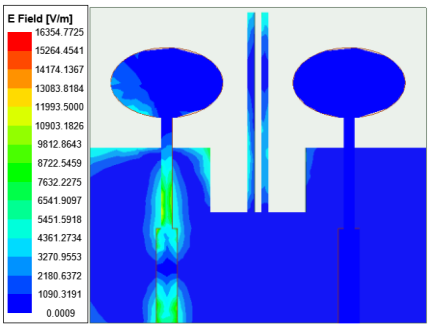

Figure 6. Surface current density.

Diversity characteristics such as ECC, DG, MEG, TARC, and CCL are considered to verify the proposed MIMO antenna's performance and capability. These characteristics are crucial MIMO diversity and multiplexing factors that assure the suggested structure's operation. The ECC which considers radiation pattern, polarization, and relative phase of the fields can be calculated using (1) [16],

$$ECC = \frac{\left|\iint_{4\pi} F_1^*(\theta,\varphi).F_2(\theta,\varphi)d\Omega\right|^2}{\iint_{4\pi}|F_1(\theta,\varphi)|^2 \times \iint_{4\pi}|F_2(\theta,\varphi)|^2 d\Omega} \quad (1)$$

The MIMO antenna's DG is determined as follows: -

$$DG = 10\sqrt{1 - ECC^2} \quad (2)$$

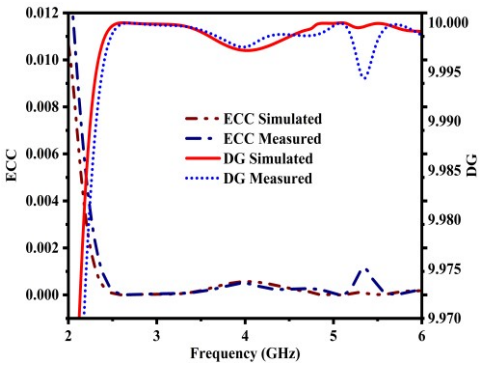

Figure 7. ECC and DG.

DG should be near to 10dB. As displayed in Figure 7, the computed ECC and DG are < 0.002 and 9.99dB, respectively, indicating good diversity performance.

TARC is a crucial metric in dual-port antennas since it shows the relationship between radiated and received power. The TARC of the two-port antenna can be determined as follows:

$$TARC = \frac{\sqrt{(S_{11}+S_{12})^2+(S_{21}+S_{22})^2}}{2} \quad (3)$$

For MIMO systems, TARC should ideally be < 0dB. The TARC has a simulated value of < 0.35, as shown in Figure 8.

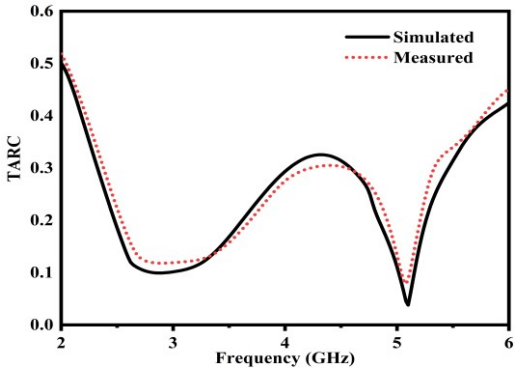

Figure 8. TARC.

MEG is a metric for calculating the median power from the event power [17]. For two element MEG can be determined using equation (4) and (5) and shown in Figure 9.

$$MEG_i = 0.5\left[1 - \sum_{j=1}^{N} |S_{ij}|^2\right] < -3dB \quad (4)$$

$$MEG_j = 0.5\left[1 - \sum_{i=1}^{N} |S_{ij}|^2\right] < -3dB \quad (5)$$

$$\left|MEG_i - MEG_j\right| < 3dB \quad (6)$$

$$\left|\frac{MEG_i}{MEG_j}\right| = \pm 3dB \quad (7)$$

Where, i and j, respectively, stand for the first and second antenna elements.

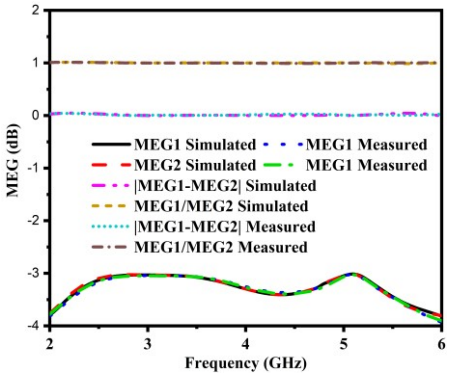

Figure 9. MEG.

CCL is calculated using equation (8) [18] for dual-element MIMO antenna, as represented in Figure 10. Practically, CCL operates at less than 0.3 bits/second/Hz.

$$CCL = -\log_2 det[\beta^R] \quad (8)$$

$$[\beta^R] = \begin{bmatrix} \beta_{ii} & \beta_{ij} \\ \beta_{ji} & \beta_{jj} \end{bmatrix}$$

$$\beta_{ii} = 1 - \left(\sum_{j=1}^{N} |S_{ij}|^2\right)$$

$$\beta_{ij} = -\left(S_{ii}^* S_{ij} + S_{ji}^* S_{ij}\right)$$

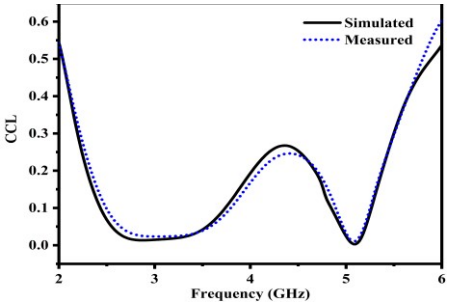

Figure 10. CCL.

Table 1: Comparative Table of Proposed mm-wave MIMO Antenna

Ref.	Dimension	Bandwidth	Edge to edge gap	Max. Isolation	ECC
[19]	78×40 mm2	2.4- 6.55 GHz (4.15 GHz)	10 mm	-35 dB	0.1
[20]	32×32 mm2	3.1-10.6 GHz (7.5 GHz)	-	-30 dB	0.02
[21]	50×30 mm2	2.5 –14.5 GHz (12 GHz)	-	-50 dB	0.04
[22]	75×150 mm2	3.3-5.0 GHz (1.7 GHz)	10 mm	-40 dB	0.05
[23]	80×80 mm2	5.71–8.2 GHz (2.41 GHz)	23.29 mm	-25 dB	0.05
[24]	50×22.5 mm2	5.23–6.42 GHz (1.19 GHz)	12.2 mm	-40 dB	0.001
This work	**48×45 mm^2**	**2.17-5.52 GHz (3.35 GHz)**	**10 mm**	**-51.15 dB**	**0.002**

The designed MIMO antenna has been compared with related works that have been recently published, and the summations are presented in Table 1. The dimension of the design antenna is 48 × 45 mm2, which is more compact than all others except [20,21,24]. However, the mutual coupling of [20,21] is higher, and ECC is larger compared to the proposed work. [24] has a larger distance between adjacent antenna's edges and lesser isolation than the proposed work. The proposed work is more isolated than any of the other antennas reported in Table 1. According to [20,21], the bandwidth is larger but at the expense of high mutual coupling and ECC. [24] has low ECC, large dimension, and low maximum isolation. Hence, the proposed I-shaped stub-based DGS approach can serve as a useful eminently usable technique for achieving efficient isolation in a MIMO antenna. It can be preferably used for C-band applications such as Bluetooth and Wi-Fi. This antenna is more isolated than any of the other antennas reported in Table 1.

IV. CONCLUSION

The designed MIMO antenna with one rectangular slot, two I-shaped Stub is small, simple, and easy to construct. Antenna edges are spaced 10 mm apart, and it is capable of delivering frequencies ranging from 2.17GHz to 5.52GHz. Two simple I-shaped stubs and a rectangular slots have been provided to reduce mutual coupling by suppressing the surface waves in desired frequency band. Maximum isolation is -51.15 dB at 2.62 GHz without deteriorating the bandwidth. This antenna exhibits good performance parameters within the required frequency range and therefore its implementation in S-band and C-band can be envisaged.

REFERENCES

[1] Chouhan S, Panda DK, Gupta M, Singhal S. Meander line MIMO antenna for 5.8 GHz WLAN application. International Journal of RF and Microwave Computer-Aided Engineering. (2018);28(4):e21222.

[2] Hampton JR. Introduction to MIMO communications. Cambridge university press; (2013).

[3] Beigi P, Rezvani M, Zehforoosh Y, Nourinia J, Heydarpanah B. A tiny EBG-based structure multiband MIMO antenna with high isolation for LTE/WLAN and C/X bands applications. International Journal of RF and Microwave Computer-Aided Engineering. (2020);30(3):e22104.

[4] Tse D, Viswanath P. Fundamentals of wireless communication. Cambridge university press; (2005).

[5] Mohammad Alibakhshikenari, Bal S Virdee, Panchamkumar Shukla, Chan H See, Raed A Abd-Alhameed, Francisco Falcone, Karim Quazzane, and Ernesto Limiti. Isolation enhancement of densely packed array antennas with periodic mtm-photonic bandgap for sar and mimo systems. IET Microwaves, Antennas & Propagation, 14(3):183–188, 2020.

[6] Mohammad Alibakhshikenari, Bal S Virdee, Chan H See, Raed A AbdAlhameed, Francisco Falcone, and Ernesto Limiti. Surface wave reduction in antenna arrays using metasurface inclusion for mimo and sar systems. Radio Science, 54(11):1067–1075, 2019.

[7] Mohammad Alibakhshikenari, Bal S Virdee, Panchamkumar Shukla, Chan H See, Raed Abd-Alhameed, Mohsen Khalily, Francisco Falcone, and Ernesto Limiti. Interaction between closely packed array antenna elements using meta-surface for applications such as mimo systems and synthetic aperture radars. Radio Science, 53(11):1368–1381, 2018.

[8] Kumar P, Sinha R, Choubey A, Mahto SK. A Novel Metamaterial Electromagnetic Band Gap (MM-EBG) Isolator to Reduce Mutual Coupling in Low-Profile MIMO Antenna. Journal of Electronic Materials. 2021:1-9.

[9] Yunqi Fu and Naichang Yuan. Elimination of scan blindness in phased array of microstrip patches using electromagnetic bandgap materials. IEEE Antennas and Wireless Propagation Letters, 3:63–65, 2004.

[10] Jeet Banerjee, Anirban Karmakar, Rowdra Ghatak, and Dipak Ranjan Poddar. Compact cpw-fed uwb mimo antenna with a novel modified minkowski fractal defected ground structure (dgs) for high isolation and triple band-notch characteristic. Journal of electromagnetic Waves and Applications, 31(15):1550–1565, 2017.

[11] Mohammad Alibakhshikenari, Bal Singh Virdee, Mohsen Khalily, Chan Hwang See, Raed Abd-Alhameed, Francisco Falcone, and Ernesto Limiti. New approach to suppress mutual coupling between longitudinal-slotted arrays based on siw antenna loaded with metal-fences working on vhf/uhf frequency-bands: study, investigation, and principle. In 2018 Asia-Pacific Microwave Conference (APMC), pages 1564–1566. IEEE, 2018.

[12] Mohammad Alibakhshikenari, Bal S Virdee, Chan H See, Raed Abd-Alhameed, Francisco Falcone, and Ernesto Limiti. Mutual-coupling reduction in metamaterial substrate integrated waveguide slotted antenna arrays using metal fence isolators for sar and mimo applications. In 2018 12th International Congress on Artificial Materials for Novel Wave Phenomena (Metamaterials), pages 013–015. IEEE, 2018.

[13] L Li, Z-L Zhou, J-S Hong, and B-Z Wang. Compact dual-band-notched uwb planar monopole antenna with modified srr. Electronics Letters, 47(17):950–951, 2011.

[14] Praveen Kumar, Rashmi Sinha, Arvind Choubey, and Santosh Kumar Mahto. A miniaturized rectangular shape narrowband mimo antenna with reduced mutual coupling for c-band applications. Journal of Electromagnetic Waves and Applications, pages 1–14, 2022.

[15] D-B Hou, S Xiao, B-Z Wang, Li Jiang, J Wang, and W Hong. Elimination of scan blindness with compact defected ground structures in microstrip phased array. IET microwaves, antennas & propagation, 3(2):269–275, 2009.

[16] A. K. Singh, S. K. Mahto, and R. Sinha, “Compact super-wideband mimo antenna with improved isolation for wireless communications,” Frequenz, vol. 75, no. 9-10, pp. 407–417, 2021.

[17] A. A. Glazunov, A. F. Molisch, and F. Tufvesson, “Mean effective gain of antennas in a wireless channel,” IET microwaves, antennas & propagation, vol. 3, no. 2, pp. 214–227, 2009.

[18] A. K. Singh, S. K. Mahto, and R. Sinha, “A miniaturized mimo antenna for c, x, and ku band applications,” Progress In Electromagnetics Research C, vol. 117, pp. 31–40, 2021.

[19] Li L, Zhou ZL, Hong JS, Wang BZ. Compact dual-band-notched UWB planar monopoleantenna with modified SRR. Electronics Letters. 2011;47(17):950-1.

[20] Ren J, Hu W, Yin Y, Fan R. Compact printed MIMO antenna for UWB applications. IEEE antennas and wireless propagation letters. 2014;13:1517-20.

[21] Iqbal A, Saraereh OA, Ahmad AW, Bashir S. Mutual coupling reduction using F-shaped stubs in UWB-MIMO antenna. IEEE access. 2017;6:2755-9.

[22] Zhao A, Ren Z. Wideband MIMO antenna systems based on coupled-loop antenna for 5G N77/N78/N79 applications in mobile terminals. IEEE Access. 2019;7:93761-71.

[23] Varshney G, Singh R, Pandey VS, Yaduvanshi RS. Circularly polarized two-port MIMO dielectric resonator antenna. Progress In Electromagnetics Research M. 2020;91:19-28.

[24] Khan I, Wu Q, Ullah I, Rahman SU, Ullah H, Zhang K. Designed Circularly Polarized Two-Port Microstrip MIMO Antenna for WLAN Applications. Applied Sciences. 2022;12(3):1068.